Load-strain-time behaviours of a PP geogrid affected by temperature change histories

Bhubehj Terum & Warat Kongkitkul
King Mongkut's University of Technology Thonburi, Thailand

ABSTRACT: Polymer geosynthetic reinforcements are presently widely adopted in the constructions of reinforced-soil (GRS) structures. The reason may attribute to their high performance-to-cost ratio. However, it is revealed in the literature that their tensile strength and deformation properties are significantly dependent on strain rate and ambient temperature. Namely, the rupture tensile strength typically increases with an increase in the strain rate, while decreases with an increase in the ambient temperature. Moreover, they also exhibit significant creep deformation upon sustained loading, and this creep deformation increases with an increase in the ambient temperature. This research explores further into the effects of temperature change history on the strength and deformation properties of a polypropylene (PP) geogrid. The study is carried out by performing tensile loading tests under different temperature and loading conditions. It is found that, under the conditions in which the ambient temperature is kept constant, or increased, or decreased during creep, the instantaneous tensile load of PP geogrid is rather a unique function of the current tensile strain, its rate, and the current temperature. The residual tensile strength is rather a unique function of strain rate and temperature at rupture. However, by cyclical change of temperature during creep, creep strain is repeatedly accelerated and decelerated, which results in a large creep strain and reduction of residual tensile strength.

Keywords: geosynthetics, creep, temperature, ageing, cyclic

1 INTRODUCTION

In the design practice of a geosynthetic-reinforced soil (GRS) structure, it is necessary to take into account deteriorations (e.g., by installation damage, chemical/biological degradation, creep) of the strength and stiffness properties of the geosynthetic reinforcement. To prevent long-term creep rupture of the geosynthetic reinforcement, it is suggested that a creep reduction factor (RF_{CR}) shall be applied (Koerner 2005; GRI 2012). RF_{CR} is evaluated from a creep rupture curve, formulated by analysing results originally from a set of conventional creep tests. These tests are, however, extremely time-consuming. As a result, a method to shorten time is proposed by performing creep test at elevated temperatures in order to accelerate the creep process. The method is called the time-temperature superposition (TTS), by which, under a set of constant but different ambient temperatures, creep tests are performed at various tensile loads until the specimen rupture. In order to alleviate the requirement of multiple replicated specimens in TTS test, a method called stepped isothermal method (SIM) was developed, by which creep test is performed under a series of stepped increased temperatures using a single specimen (Thornton et al. 1998). From a number of SIM test results found in the literature, it is revealed that, with an increase in the ambient temperature, rupture tensile strength and stiffness of geosynthetic reinforcement decrease, while the tensile strain at rupture increases. It seems that the load-strain-time behaviours of geosynthetic reinforcement is subjected to changes in the ambient temperature (e.g., increasing, decreasing, cyclically change), and its effects can be significant to the performance of GRS structures, which are subjected to temperature change.

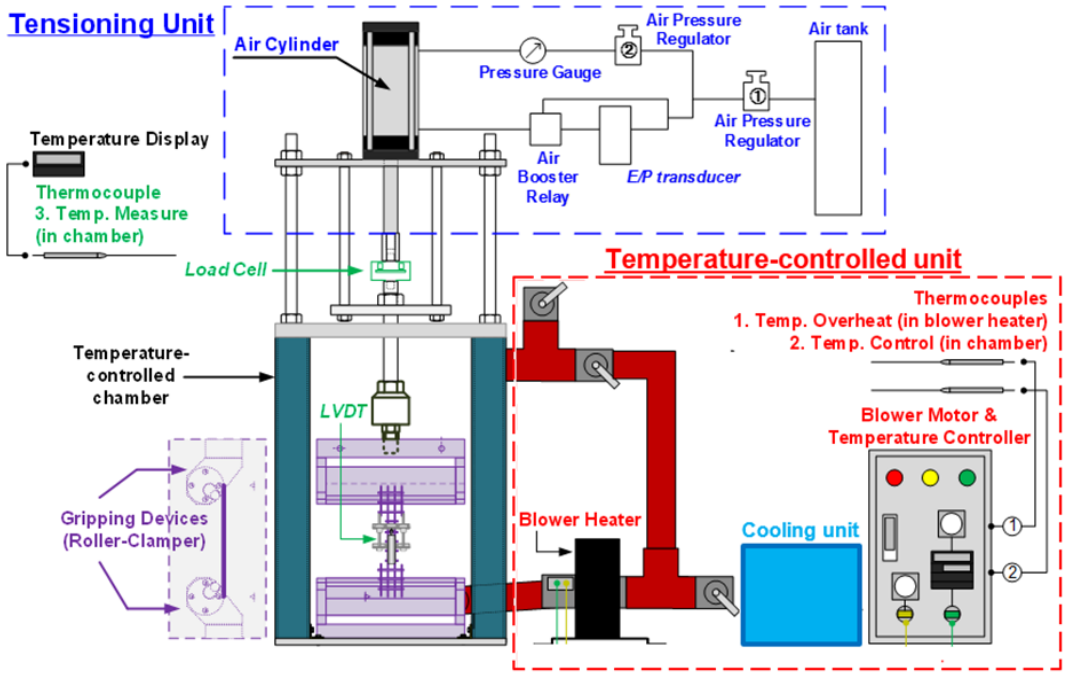

Figure 1. Details of tensioning and temperature-controlled units of the tensile loading apparatus (modified from Kongkitkul et al. 2012)

To study the effects of temperature change histories on load-strain-time behaviours of geosynthetic reinforcement, a special series of tensile loading tests were performed on a type of polypropylene (PP) geogrid. The followings loading and temperature histories are employed in the present study: 1) monotonic loading under constant temperature; 2) sustained loading under constant temperature; 3) sustained loading under increasing temperature; 4) sustained loading under decreasing temperature; and 5) sustained loading with cyclically changed temperature.

2 APPARATUS AND MATERIAL

2.1 *Tensioning and temperature-controlled units*

A tensile loading apparatus, which is of load-controlled type, was used. The tensioning unit consists of a double-action air cylinder, an electro-pneumatic (EP) transducer and a personal computer. By using this apparatus, the load rate can be accurately controlled by the computer and the sustained loading (SL) can be successfully performed using the feedback from the load cell. On the other hand, the temperature in the test chamber can be successfully controlled by the network of hot air flow. The working principles of the temperature-controlled unit are as follows. Fresh room-temperature air is supplied to the blower and then transferred to the heater. Hot air is provided to the chamber via an air pipe arranged at the bottom, and moves inside a perforated air pipe arranged inside the chamber. The heat from the hot air is well distributed by means of a set of fans in the chamber. The hot air exits from the top of the chamber. Half of this exited area is circulated to mix with fresh air before entering to the blower again. For testing with decreasing temperature, the fresh air is cooled down first by a cooling unit before entering to the blower. Figure 1 shows the details of loading and temperature-controlled units used in the present study.

2.2 *Measuring device*

Tensile load axially applied to a specimen was measured by a load cell. It is connected to the loading piston as shown in Figure 1. A miniature frame was installed at the centre part of the specimen to measure locally the specimen's deformation by a displacement sensor attached on.

2.3 *Test material*

A PP geogrid was used in this study. It is a biaxial geogrid type. The aperture shape of this geogrid is square and the size is 35 mm wide (centre-to-centre) in both longitudinal and transverse directions.

Table 1. Summary of rupture tensile strength, rupture tensile strain, and tensile stiffness for different ambient temperatures in ML-CT and ML-VT tests.

ML-CT tests					ML-VT tests					
T (°C)	$V_{max,cor}$ (kN/m)	ε_{rup} (%)	$E_{2\%}$ (kN/m)	$E_{5\%}$ (kN/m)	T (°C)	SL. time (hr)	$V_{max,cor}$ (kN/m)	ε_{rup} (%)	$E_{2\%}$ (kN/m)	$E_{5\%}$ (kN/m)
30	44.99	9.82	617.03	501.12	40-30	1	44.03	8.93	586.64	479.11
35	41.20	10.29	602.21	463.54		3	43.78	8.95	552.86	470.02
40	39.42	10.52	533.05	421.17	50-30	1	42.44	8.27	592.56	488.48
45	34.39	11.81	453.58	361.93		3	42.58	7.72	556.37	485.27
50	30.52	12.87	431.37	338.72						

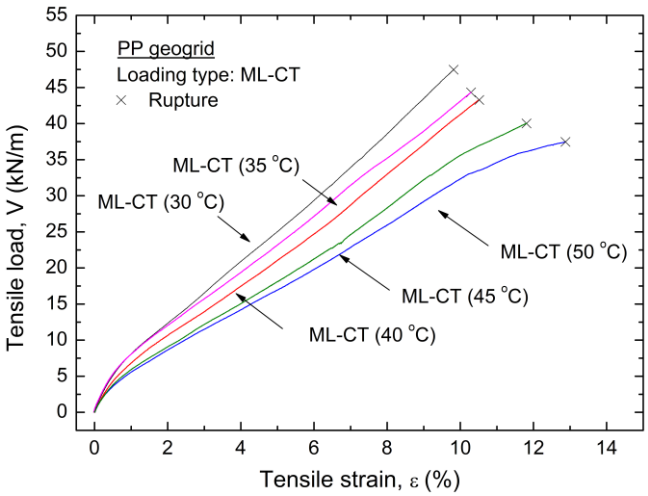

Figure 2. Tensile load – tensile strain relations from ML-CT tests

3 TEST PROGRAM

In this study, the following six different loading and temperature histories are employed:

1. Monotonic Loading-Constant Temperature (ML-CT): continuous monotonic loading (ML) is performed at a constant load rate of 0.6 kN/m/min towards the specimen's rupture. The ambient temperature is kept constant at either 30 °C, 35 °C, 40 °C, 45 °C or 50 °C throughout each test.
2. Monotonic Loading- Variant Temperature (ML-VT): heat is applied to specimen at the temperature of either 40 °C or 50 °C under zero tensile load for designated time of either 1 hr or 3 hrs, then temperature is reduced to 30 °C. After that, continuous ML at the temperature of 30 ° until the specimen's rupture.
3. Sustained Loading-Constant Temperature (SL-CT): the ambient temperature is controlled constant either at 30 °C, 40 °C or 50 °C, throughout each test. ML is performed at a constant load rate of 0.6 kN/m/min until the tensile load is equal to the designated value for performing SL. SL is performed for a period of three hours, followed by the restart of ML at the original load rate until the specimen's rupture.
4. Sustained Loading-Increase Temperature (SL-IT): this loading type is similar to SL-CT in that SL test for three hours that is followed by ML towards the specimen's rupture is performed. However, the temperature during SL is increased from 30 °C to 40 °C or 30 °C to 50 °C during SL test.
5. Sustained Loading-Decrease Temperature (SL-DT): this loading type is similar to SL-CT in that SL test for seven hours that is followed by ML towards the specimen's rupture is performed. However, the temperature during SL is reduced from 50 °C to 30 °C during SL test.
6. Sustained Loading-Cyclic Temperature (SL-CYT): this loading type is similar to SL-CT in that SL test for 36 hours that is followed by ML towards the specimen's rupture is performed. However, the temperature during SL is cyclically changed between 50 °C and 30 °C during SL test.

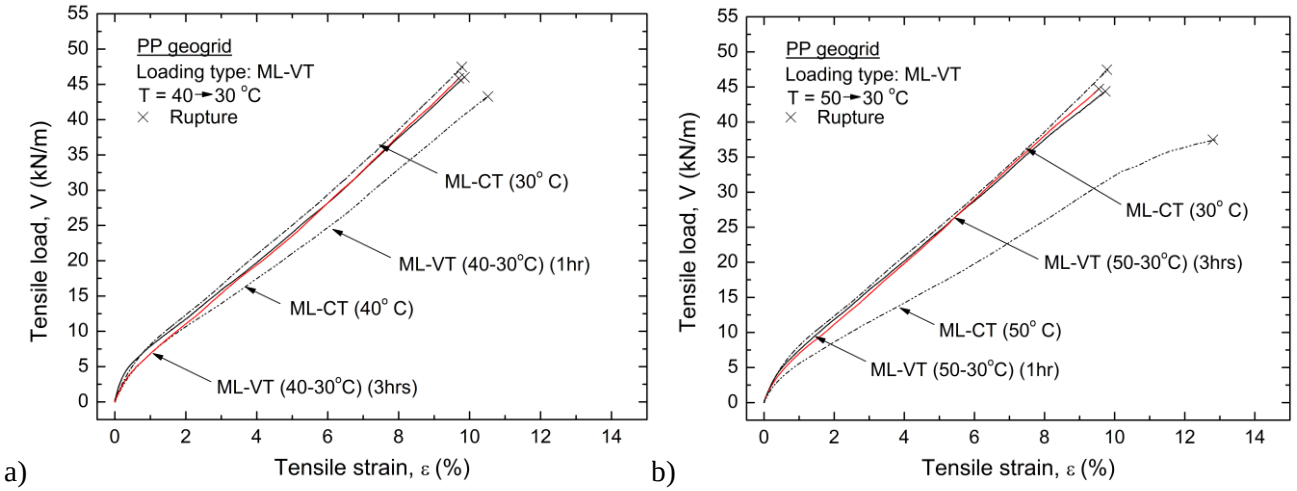

Figure 3. Tensile load – tensile strain relations from ML-VT tests: a) ML-VT (40-30 °C); and b) ML-VT (50-30 °C), in comparison with ML-CT tests at T = 30, 40, and 50 °C

4 RESULT AND DISSCUSSION

4.1 *Effect of temperature on rupture strength*

Figure 2 shows relationships between tensile load (V) and tensile strain (ε) from ML-CT tests. Due to tangent stiffness of V-ε relation varies while the load rate used to perform these tests is the same, the strain rate at rupture for different V-ε relations in Figure 2 are different. The measured rupture tensile strength (V_{max}) was corrected to values at the same strain rate of 0.1 %/min (selected as a reference strain rate) (Kongkitkul et al. 2012). Table 1 summarises the corrected V_{max} ($V_{max,cor}$), rupture strain (ε_{rup}) and tensile stiffnesses defined at ε values equal to 2% and 5% ($E_{2\%}$ and $E_{5\%}$) for different ambient temperatures. It can be seen that, with an increase in the ambient temperature from 30 °C, the values of $V_{max,cor}$ and $E_{2\%}$ and $E_{5\%}$ decrease significantly while the ε_{rup} increases.

4.2 *Effect of temperature change with no tension*

Figures 3a and 3b show V-ε relations from ML-VT tests for the maximum applied temperatures with no tension of 40 °C and 50 °C, respectively. Table 1 also summarises $V_{max,cor}$, ε_{rup}, and $E_{2\%}$ and $E_{5\%}$ values from ML-VT tests for different maximum previous temperatures applied to the specimens with no tension. It is to be noted that the temperature is kept constant at 30 °C during the application of ML until specimen's rupture. It can be observed that the V-ε relations from ML-VT (50-30 °C) and ML-VT (40-30 °C) tests with different periods of exposure (i.e., 1 hr and 3 hrs) to the increased temperatures (40 °C or 50 °C) are significantly similar to the one obtained by ML-CT (30 °C). The values of $V_{max,cor}$ for ML-VT (50-30 °C) and ML-VT (40-30 °C) tests are significantly similar to each other, while they are slightly lower than the value observed in ML-CT (30 °C) test. Thus, increasing the ambient temperature to 40 °C or 50 °C while keeping no tension to the PP geogrid does not significantly change the strength and stiffness properties of PP geogrid.

4.3 *Creep deformation characteristics*

Figures 4a, 4b and 4c show V-ε relations that are obtained from SL-CT tests at constant temperatures of 30, 40 and 50 °C, respectively. It can be seen from each figure that noticeable creep developed during SL stage in the SL-CT tests and the amount of creep increases with an increase in the tensile load at which SL was performed. In each figure, upon the start of ML at the ends of SL, the V-ε relations by SL-CT tests show significantly high stiffness after which they tend to rejoin to the V-ε relation by ML-CT test until specimen's rupture. It could be also seen that, with the intermission of SL in SL-CT tests, despite the development of creep strain, the residual tensile strength is maintained to be similar to the rupture tensile strength by ML-CT tests. That is, creep strain developed under elevated constant temperatures is not a degrading phenomenon. In addition, any interaction between creep strain and increased temperature seems to be insignificant.

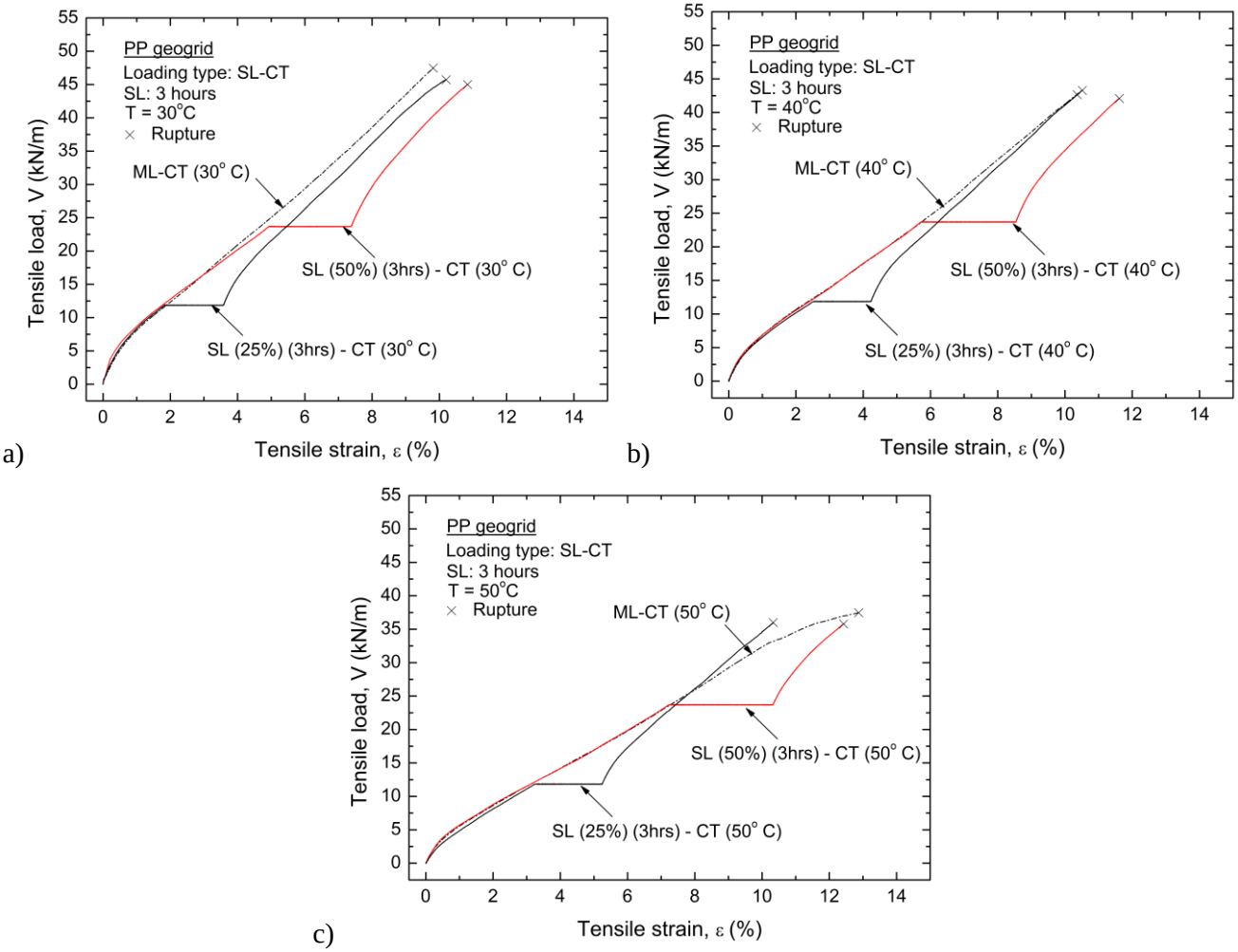

Figure 4. Tensile load – tensile strain relations from SL-CT tests: a) SL-CT (30 °C); b) SL-CT (40 °C); and c) SL-CT (50 °C)

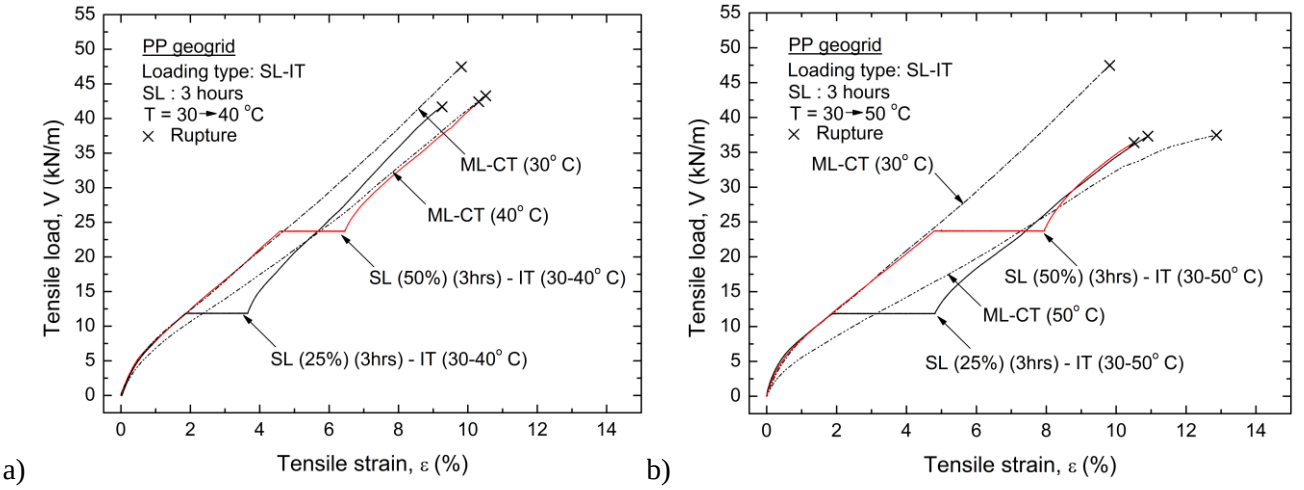

Figure 5. Tensile load – tensile strain relations from SL-IT tests: a) SL-IT (30-40 °C); and b) SL-IT (30-50 °C), in comparison with ML-CT tests at T = 30, 40, and 50 °C

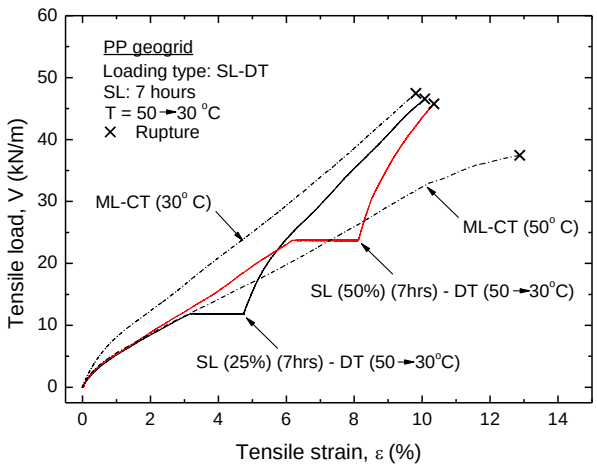

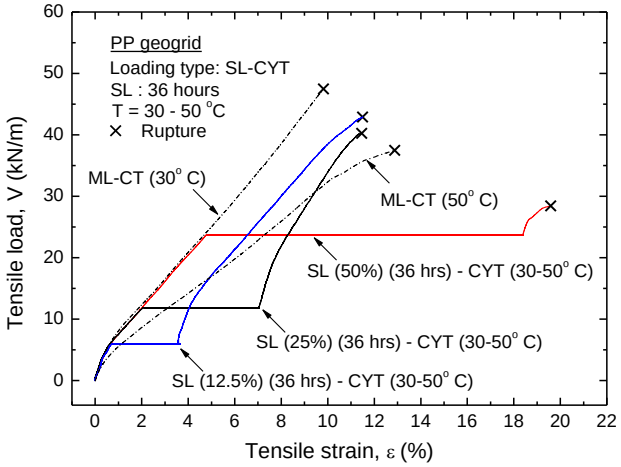

Figure 6. (Left) Tensile load – tensile strain relations from SL-DT (50-30 ºC) tests, in comparison with ML-CT tests at T = 30 and 50 ºC

Figure 7. (Right) Tensile load – tensile strain relations from SL-CYT (30-50 oC) tests, in comparison with ML-CT tests at T = 30 and 50 oC

Figures 5a and 5b show the V-ε relations that obtained from SL-IT tests for the ambient temperature during SL that was increased from 30-40 ºC and 30-50 ºC, respectively. It can be seen that the creep strain was accelerated during SL by increasing temperature from 30 to 40 ºC (cf. Figs. 5a and 4a) and from 30 to 50 ºC (cf. Figs. 5b and 4a). For the same elapsed time during SL, the amount of creep strain becomes greater with how much the temperature was increased during the SL course (cf. Figs. 5a and 5b). Upon the start of ML at the end of SL in SL-IT tests, the V-ε relations show a high stiffness behaviour, and then rejoin to the ones by ML-CT tests for the same temperatures. It could be seen also that the residual tensile strengths observed with SL-IT tests are significantly similar to the corresponding rupture tensile strengths by ML-CT tests. Moreover, any interaction between creep straining and increasing temperature during the SL course seems to be insignificant.

Figure 6 shows the V-ε relations that obtained from SL-DT (50-30 ºC) tests. It can be seen that the creep strain during the SL course is decelerated as, at the same tensile load, the amount of creep strain by SL-DT (50-30 ºC) tests is less than the one by SL-CT (50 ºC) (cf. Fig. 6 and Fig. 4c). Furthermore, it is of great interest that, upon the start of ML that follows SL, the V-ε relations tend to rejoin to the one by ML-CT (30 ºC), showing that the residual tensile strength is maintained similar to the rupture tensile strength. By comparing Figs. 6 and 5b, it can be seen that negative ageing effect by increasing of temperature during SL in SL-IT (30-50 ºC) test is reversed to positive ageing effect by decreasing of temperature during SL in SL-DT (50-30 ºC) test.

Figure 7 shows the V-ε relations that are obtained from SL-CYT tests, in which the ambient temperature was changed cyclically between the lower value of 30 ºC and the upper value of 50 ºC during the SL course. The ambient temperature was changed for 6 cycles (for a total period of 36 hrs), while keeping the tensile load constant at either 12.5 %, 25 % and 50 % of $V_{max,cor}$ by ML-CT (30 ºC) test. Unlike the behaviours seen with SL-CT, SL-IT and SL-DT tests (Figs. 4 – 6), it seems that, during SL, there was an interaction between creep straining and cyclical change in the temperature, as can be seen by a greater amount of developed creep strain when compared with SL-IT test results (cf. Fig. 7 and 5b). In particular, with a high tensile load for SL (50 % in Fig. 7), it could be seen that not only creep strain was noticeably accelerated but also the residual tensile strength was significantly reduced by this cyclically change in the ambient temperature. Nevertheless, with lower tensile loads for SL (12.5 and 25 % in Fig. 7), though the creep strain is still noticeably accelerated, the residual tensile strengths were not reduced as large as with SL-CYT test at SL of 50 % of $V_{max,cor}$. The difference between the behaviours the first pattern observed with SL-CT, SL-IT and SL-DT, and the second pattern observed with SL-CYT is still not known to the best of the authors' knowledge. Further studies are necessary.

4.4 *Effects of temperature on creep strain*

As a load-controlled tensioning unit was used in the present study, the strain rate at the starts of different SL stages were different due to difference in the tangent stiffness of V-ε (by different load levels and by different temperatures) at which SL starts. For rigorous comparing among different loading and tempera-

ture schemes, the creep strains (ε_{cr}) that develop until the end of SL stages were corrected to share a selected common initial strain rate of 0.04 %/min. Figure 8 compares the values of ε_{cr} that have been corrected for the initial strain rate among different loading and temperature schemes. The following trends of

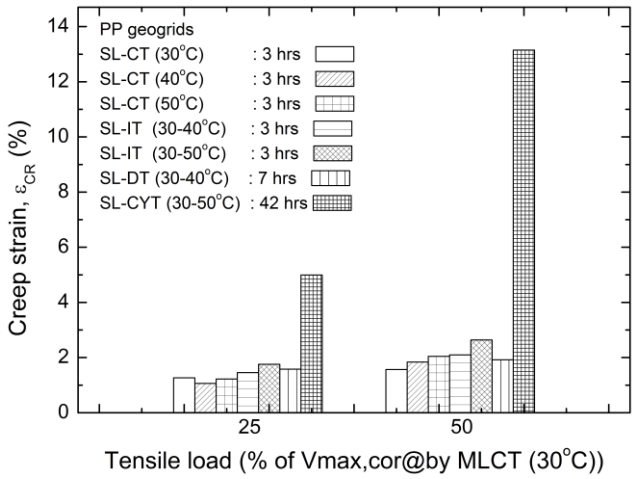

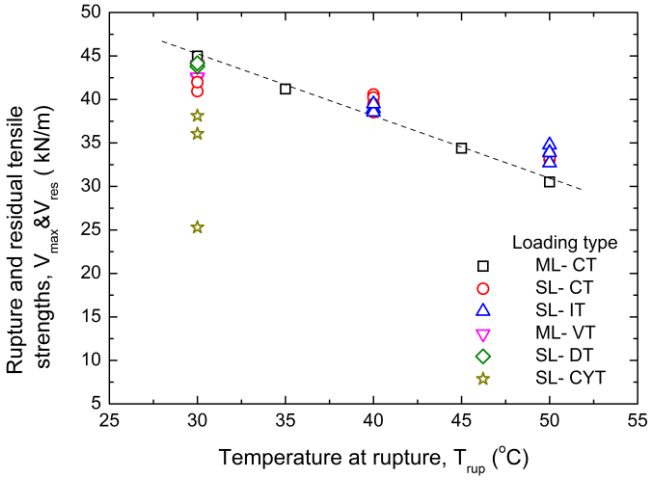

Figure 8. (Left) Comparison of creep strains developed by SL with different temperature schemes
Figure 9. (Right) Rupture tensile load vs. rupture temperature of PP geogrid

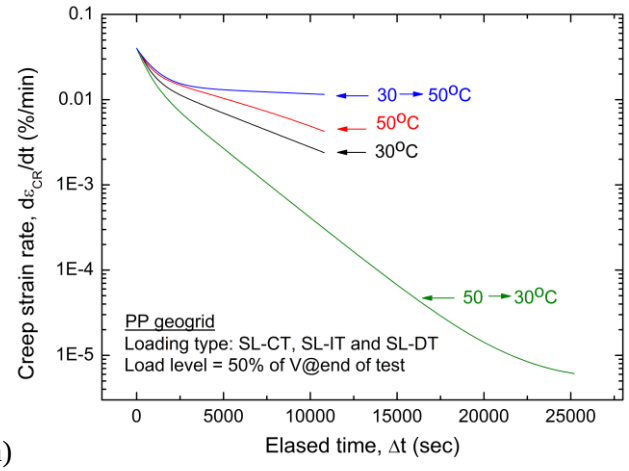

a)

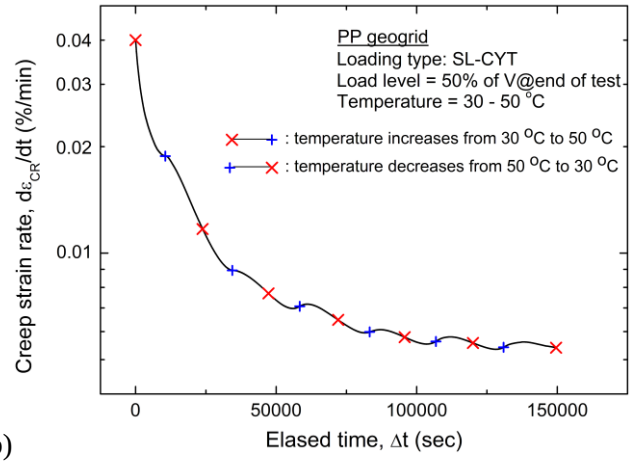

b)

Figure 10. Creep strain rate vs. time from: a) SL-CT, SL-IT and SL-DT tests; and b) SL-CYT test, tensile load during SL is 50 % of $V_{max,cor}$ by ML-CT test at 30 °C

behaviour may be observed.

1. For SL-CT tests, the value of ε_{cr} increases with an increase in the ambient temperature and the tensile load at which SL is performed. This behaviour is associated with a decrease in the stiffness (Table 1) with an increase in the temperature and tensile load, as can be seen in ML-CT tests at different temperatures (Fig. 2).
2. For the same tensile load, the value of ε_{cr} by SL-IT tests, in which the temperature was increased from 30 °C to 50 °C, is significantly larger than the values observed by SL-CT tests, in which the temperatures were held constant throughout the test at either 30 °C or 50 °C.
3. For the same tensile load, the value of ε_{cr} by SL-IT tests, in which the temperature was increased from 30 °C to 50 °C, is greater than the value by SL-DT tests, in which the temperature was reduced from 50 °C to 30 °C. This shows that the creep strain is accelerated and decelerated by increasing and decreasing the ambient temperature during SL.
4. The value of ε_{cr} by SL-CYT tests is the greatest among all the loading and temperature schemes employed. It seems that significant interaction was developed between creep straining and cyclically change in the temperature.

Observations 1) to 3) are due to the viscous property of polymer geogrid coupled with temperature effects, while without any interaction between them, and can be explained by a non-linear three-component model taking into account not only the viscous property and the temperature effects on the inviscid (plas-

tic) property (Kongkitkul and Tatsuoka 2007). Further study is necessary for modelling of the observation 4) seen in SL-CYT tests.

Figure 10a compares time histories of creep strain rate ($d\varepsilon_{cr}/dt$) during SL at the tensile load of 50 % of $V_{max,cor}$ by ML-CT test at T = 30 ^{o}C between SL-CT, SL-IT and SL-DT tests. It may be seen that, by SL-CT tests, the $d\varepsilon_{cr}/dt$ value continuously decreases with time to a value much lower than its initial value. In contrast, by SL-IT test, the $d\varepsilon_{cr}/dt$ value initially decreases with time at a high rate. Later on, it slightly decreases with time, and at the end of SL stage, it is significantly higher than those of SL-CT tests at T = 30 and 50 ^{o}C. This shows that, during SL in a SL-IT test, creep strain is accelerated by increasing temperature. On the other hand, by SL-DT test, the $d\varepsilon_{cr}/dt$ value continuously decreases with time toward a much lower value than those of SL-CT tests at T = 30 and 50 ^{o}C at their ends. This shows that, during SL in a SL-DT test, creep strain is decelerated by decreasing temperature. Figure 10b shows time history of $d\varepsilon_{cr}/dt$ during SL in a SL-CYT test at the tensile load of 50 % of $V_{max,cor}$ by ML-CT test at T = 30 ^{o}C. It may be seen that $d\varepsilon_{cr}/dt$ - time relation exhibits discontinuous decreases in the creep strain rate when the temperature increases or decreases between 30 ^{o}C and 50 ^{o}C. It could be seen that creep strain was accelerated and decelerated when the temperature increases from 30 to 50 ^{o}C and decreases from 50 to 30 ^{o}C, respectively. With the complicated temperature history in SL-CYT test, the instantaneous creep strain rate is not a unique function of current load, strain and temperature, but it is controlled by loading and temperature histories.

4.5 *Effects of loading and temperature history on rupture strength*

Figure 9 compares the rupture tensile strengths (V_{max}) from ML-CT tests and the residual tensile strength (V_{res}) from SL-CT, SL-IT, ML-VT, SL-DT, and SL-CYT tests at various temperatures at rupture (T_{rup}). A line was best fitted to the V_{max} - T_{rup} data points from ML-CT tests. It may be seen that, for the same temperature at rupture, the values of V_{res} from ML-VT, SL-CT, SL-IT and SL-DT tests are significantly similar to V_{max} from ML-CT tests. Contrary, the values of V_{res} from SL-CYT tests are noticeably lower than the corresponding V_{max} value. Thus, for cyclically change in the temperature during SL, the V_{res} is additionally dependent on the applied temperature history.

5 CONCLUSION

The following conclusions can be derived from the test results described in the present study.

1. With an increase in the ambient temperature, the creep strain of PP geogrid increases while the rupture tensile strength and stiffness decrease.
2. Under the conditions in which the ambient temperature is kept constant, or increased, or decreased during creep, the instantaneous tensile load of PP geogrid is rather a unique function of the current tensile strain, its rate, and the current temperature. The residual tensile strength is rather a unique function of strain rate and temperature at rupture.
3. Upon the cyclically change in the ambient temperature while sustained loading to PP geogrid, the creep strain rate was accelerated and decelerated by increasing and decreasing the ambient temperature, respectively. This results in a large accumulated creep strain and the reduction of residual tensile strength. It seems that there is an interaction between creep straining and cyclical change of the ambient temperature during creep. Further study is necessary to understand this behaviour.

REFERENCES

Koerner RM. 2005. Designing with Geosynthetics. Pearson Education, Inc., ch. 3, New Jersey, USA.

Geosynthetic Institute 2012. Determination of the Long-Term Design Strength of Stiff Geogrids. GRI Standard Practice GG4(a).

Geosynthetic Institute 2012. Determination of the Long-Term Design Strength of Flexible Geogrids. GRI Standard Practice GG4(b),

Thornton JS, Paulson JN, and Sandri D 1998. Conventional and Stepped Isothermal Methods for characterizing long term creep strength of polyester geogrids. in Proc. 6th Int. Conf. on Geosynthetics, pp. 691-698.

Hirakawa D, Kongkitkul W, Tatsuoka F, and Uchimura T 2003. Time-dependent stress-strain behaviour due to viscous properties of geogrid reinforcement. Journal of Geosynthetics International. 10, pp. 176-199.

Kongkitkul W, Tabsombut W, Jaturapitakkul C and Tatsuoka F 2012. Effects of temperature on the rupture strength and elastic stiffness of geogrids. Geosynthetics International, 19, No. 2, 106-123.

Tatsuoka F, Benedetto D, Kongkitkul W, Kongsukprasert L, Nishi T and Sano Y 2008. Modelling of ageing on the elasto-viscoplastic behaviour of geomaterial. J. of Soils and Foundations, Vol. 48, pp. 155-174.
Kongkitkul W and Tatsuoka F 2007. A theoretical framework to analyse the behaviour of polymer geosynthetic reinforcement in temperature accelerated creep tests. J. of Geosynthetics International, Vol. 14, pp. 23-38.